Development of Graphical Methods for Estimating the Diffusivity Coefficient of Gases in Bitumen from Pressure-Decay Data

ARTICLE *in* ENERGY & FUELS · AUGUST 2005

Impact Factor: 2.79 · DOI: 10.1021/ef050057c

3 AUTHORS, INCLUDING:

Hussain Sheikha
Denbury Resources
10 PUBLICATIONS **83** CITATIONS
SEE PROFILE

Anil K Mehrotra
The University of Calgary
160 PUBLICATIONS **2,349** CITATIONS
SEE PROFILE

Development of Graphical Methods for Estimating the Diffusivity Coefficient of Gases in Bitumen from Pressure-Decay Data

Hussain Sheikha, Mehran Pooladi-Darvish,* and Anil K. Mehrotra

Department of Chemical and Petroleum Engineering, University of Calgary, Calgary, Alberta, Canada T2N 1N4

Received March 7, 2005. Revised Manuscript Received June 26, 2005

New graphical techniques are presented for estimating the diffusivity coefficient (or mass diffusivity) of CO_2, CH_4, and N_2 in highly viscous bitumens from pressure-decay data. These methods are based on modeling the rate of change in system pressure as gas diffuses into the bitumen using the diffusion equation, coupled with a mass balance for the gas phase. Analytical solutions of the resulting set of equations, with appropriate initial and boundary conditions, are obtained by Laplace transformation. An inverse solution technique is used for developing two graphical methods to estimate the diffusivity coefficient from pressure-decay data reported in the literature. The estimated diffusivity coefficients for gas−bitumen pairs at 75−90 °C vary from 2.5×10^{-10} m^2/s to 7.8×10^{-10} m^2/s, and these are in good agreement with literature values. The novelty of the proposed methodology is in its simplicity and its ability to isolate portions of the pressure-decay data that are affected by experimental fluctuations. This enables the consideration of only that portion of the data that is consistent with the analytical solution.

Introduction

Because of the rapid decline in conventional oil reserves, bitumens from the vast oil sands reserves in Alberta, Canada, represent an emerging source of hydrocarbons and energy. In 2003, for the first time, the bitumen production surpassed the production of conventional crude oil in Alberta.[1] The major obstacle to economic recovery and processing of bitumens is their high viscosity, making them essentially immobile at reservoir temperatures. However, the viscosity of bitumens and heavy oils can be decreased dramatically by mixing them with solvents or light gases at high pressures. The decrease in bitumen viscosity is related to the gas solubility.[2] For example, carbon dioxide with a high solubility causes a large reduction in the bitumen viscosity. The decrease in bitumen viscosity results in its improved flow and hydrocarbon recovery factors. In fact, this is the basis of an in situ recovery technique known as the VAPEX process.[3]

Molecular diffusion has an important role in the recovery processes, as well as in many other reservoir engineering applications. Therefore, an accurate value of the diffusion coefficient of gases in bitumens is essential for calculating the rate of gas dissolution in bitumens and heavy oils. An order-of-magnitude calculation for the diffusion in liquids can be obtained by two theories: the Hydrodynamic theory and the Eyring theory.[4] However, the simplifying approximations involved in these theories may not apply to the complex multiring naphthenic and aromatic molecules present in bitumens. A predictive method, based on the thermodynamic framework of the corresponding states for the diffusion coefficient of carbon dioxide in Athabasca bitumen, has been reported.[5]

The different experimental methods for the determination of the diffusivity of gases in bitumens can be broadly classified into direct and indirect methods. The direct methods, which are based on the determination of the composition of the diffusing species along the length of the bitumen sample with time, require compositional analysis.[6] However, the direct methods have a tendency to be expensive and time-consuming. On the other hand, the indirect methods measure the change in one of the system parameters that varies because of the diffusion, without the need to determine the composition. Such parameters include pressure, interface velocity, magnetic field strength, or the volume of the diffusing solute.

Grogan and Pinczewski[7] measured the diffusivity coefficient of carbon dioxide in oil and oil shielded by

* Corresponding author. Phone: (403) 220-8779. Fax: (403) 284-4852. E-mail address: pooladi@ucalgary.ca.

(1) Barter, D. Crude Bitumen Production Exceeds Conventional by 50%, Alberta Energy and Utilities Board (EUB), Calgary, Alberta, Canada, 2004.

(2) Mehrotra, A. K. Mixing Rules for Predicting the Viscosity of Bitumens Saturated with Pure Gases. *Can. J. Chem. Eng.* **1992**, *70*, 165.

(3) Butler, R. M.; Mokrys, I. J. A New Process (VAPEX) for Recovering Heavy Oils using Hot Water and Hydrocarbon Vapor. *J. Can. Pet. Technol.* **1991**, *30* (1), 97.

(4) Bird, R. B.; Stewart, W. E.; Lightfoot, E. N. *Transport Phenomena*; Wiley: New York, 2002.

(5) Mehrotra, A. K.; Garg, A.; Svrcek, W. Y. Prediction of Mass Diffusivity of CO_2 into Bitumen. *Can. J. Chem. Eng.* **1987**, *65*, 826.

(6) Schmidt, T. Mass Transfer by Diffusion. In *AOSTRA Handbook on Oil Sands, Bitumens and Heavy Oils*; Hepler, L. G.; Hsi, C., Eds.; Alberta Oil Sands Technology & Research Authority (AOSTRA): Edmonton, Alberta, Canada, 1989; Chapter 12.

(7) Grogan, A. T.; Pinczewski, W. V. The Role of Molecular Diffusion Processes in Tertiary CO_2 Flooding. *J. Pet. Technol.* **1987**, *39* (5), 591.

10.1021/ef050057c CCC: $30.25
Published on Web 08/05/2005

water, by tracking the observed interface motion and comparing it with a numerical model that was developed for the same purpose. Renner[8] determined the diffusivity coefficient by measuring the volume of dissolved gas in the liquid phase with time at constant pressure. Riazi[9] developed a model to estimate the gas diffusivity coefficient from the gas/liquid interface position and gas pressure in a constant-volume cell. Zhang et al.[10] measured the decrease in the pressure of a constant volume of gas as it diffused into the underlying bitumen. Their approach is based on a simplified version of Riazi's method,[9] which did not require the measurement of the interface position with time.

Upreti and Mehrotra[11,12] developed a numerical technique to obtain the diffusivity coefficient as a function of concentration. They obtained the diffusivity from the transient data obtained from the pressure-decay of a constant volume of gas as it dissolved into the bitumen. The diffusivity coefficients of methane, ethane, carbon dioxide, and nitrogen in two bitumen samples were provided at 25−90 °C at pressures up to 8 MPa.[11,12] Civan and Rasmussen[13,14] developed a mathematical model for the experimental setup of Zhang et al.[10] to estimate the gas diffusivity coefficient. Yang and Gu[15] presented an experimental method, along with a computational scheme, for measuring the diffusion coefficient of a solvent in heavy oil, using the dynamic pendant drop shape analysis. Tharanivasan et al.[16] studied the effect of different interface mass-transfer models to estimate the solvent diffusivity in heavy oil from the pressure-decay measurements of Zheng et al.[10] They showed that the experimental data could be matched by different interface mass-transfer models, leading to a range of diffusion coefficient values.

The objective of the present work is to develop simple methods for the determination of gas diffusivity coefficient from pressure-decay data. A mathematical model is developed based on the Fick's second law of diffusion and a mass balance for the diffusing gas. From this mathematical model, two graphical methods are derived for estimating the diffusivity coefficient using pressure-decay measurements. Specifically, the experimental pressure-decay data of Upreti and Mehrotra[11,12] are used for the determination of diffusion coefficient of three gases, namely, methane, nitrogen, and carbon dioxide in Athabasca bitumen.

The experimental protocol of Upreti and Mehrotra[11,12] is described briefly in the following section, which is followed by the development of the mathematical model for the change in the pressure of the gas on top of the bitumen as diffusion progresses. The development of the inverse solution methodology for interpreting experimental data is given subsequently, followed by the results obtained from this study.

Pressure-Decay Data

The experimental setup developed by Upreti and Mehrotra[11,12] consisted of a pressure cell placed in a constant-temperature water bath for isothermal diffusion experiments. In each pressure-decay experiment, a constant amount of gas filled the top 2 cm of the pressure cell, while the lower 1 cm was filled with a sample of Athabasca bitumen. The preheating coil and the pressure cell were submerged completely in the water bath and placed on an air cushion to make it vibration-free. The cell pressure was measured continuously using a quartz pressure-sensing instrument with high accuracy. The pressure cell was filled with a layer of bitumen ~1 cm thick and the mass of the bitumen was recorded. The cell was then placed inside the constant-temperature water bath. The air was purged from the cell after the bitumen attained the bath temperature. The test gas was introduced quickly into the cell, and the pressure was increased to the initial test pressure. The pressure was then recorded as the gas diffused into the bitumen. Further details of the experimental apparatus and procedure for the pressure-decay tests were given by Upreti and Mehrotra.[11,12]

Two samples of Athabasca bitumen were used in the pressure-decay experiments:[11,12] the SCF bitumen from Suncor's Coker Feed and the SYN bitumen from Syncrude in Fort McMurray, Alberta, Canada. The viscosities of the SCF and SYN bitumen samples at 40 °C were ~35 and 106 Pa s , respectively, and the densities of the SCF and SYN bitumen samples at 40 °C were ~995 and 1010 kg/m^3, respectively.[11,12] The isothermal pressure-decay tests were performed with methane, ethane, carbon dioxide, and nitrogen at different temperatures and (initial) pressures.[11,12]

Mathematical Model: The Forward Problem

There are two important parameters governing the diffusion process in the pressure-decay experiments of Upreti and Mehrotra.[11,12] One is the gas solubility, which controls the amount of gas that is dissolved at the gas/bitumen interface and determines the driving force for gas diffusion in the bulk. The gas solubility also determines the amount of gas that could eventually dissolve in the bitumen after a long time. The second parameter is the diffusion coefficient, which controls the rate of mass transfer by molecular diffusion within the bitumen phase.

As stated previously, the main purpose of this paper is to develop a simple method(s) for the estimation of

(8) Renner, T. A. Measurement and Correlation of Diffusion Coefficients for CO_2 and Rich-Gas Applications. *SPE Res. Eng.* **1988**, *3*, 517.

(9) Riazi, M. R. A New Method for Experimental Measurement of Diffusion Coefficients in Reservoir Fluids. *J. Pet. Sci. Eng.* **1996**, *14*, 235.

(10) Zhang, Y.; Hyndman, C. L.; Maini, B. Measurement of Gas Diffusivity in Heavy Oils. Presented at 49th Annual Technical Meeting of the Petroleum Society of CIM, Calgary, Alberta, Canada, June 8−10, 1998, Paper 98-63.

(11) Upreti, S. R.; Mehrotra, A. K. Experimental Measurement of Gas Diffusivity in Bitumen: Results for Carbon Dioxide. *Ind. Eng. Chem. Res.* **2000**, *39*, 1080.

(12) Upreti, S. R.; Mehrotra, A. K. Diffusivity of CO_2, CH_4, C_2H_6 and N_2 in Athabasca Bitumen. *Can. J. Chem. Eng*. **2002**, *80*, 116.

(13) Civan, F.; Rasmussen, M. L. Accurate Measurement of Gas Diffusivity in Oil and Brine under Reservoir Conditions. Presented at SPE Mid Continent Operations Symposium, Oklahoma City, OK, March 24−27, 2001, SPE Paper No. 67319.

(14) Civan, F.; Rasmussen, M. L. Improved Measurement of Gas Diffusivity for Miscible Gas Flooding under Nonequilibrium vs Equilibrium Conditions. Presented at SPE/DOE Improved Oil Recovery Symposium, Tulsa, OK, April 13−17, 2002, SPE Paper No. 75135.

(15) Yang, C.; Gu, Y. A New Method for Measuring Solvent Diffusivity in Heavy Oil by Dynamic Pendant Drop Shape Analysis (DPDSA). Presented at SPE Annual Technical Conference and Exhibition, Denver, CO, October 5−8, 2003, SPE Paper No. 84202.

(16) Tharanivasan, A. K.; Yang, C.; Gu, Y. Comparison of Three Different Interface Mass Transfer Models used in the Experimental Measurement of Solvent Diffusivity in Heavy Oil. *J. Pet. Sci. Eng.* **2004**, *44*, 269.

diffusivity coefficients. The approach involves the development of an analytical solution for the gas pressure, which can then be inverted to find the diffusion coefficient. An analytical model is developed using a few simplifying assumptions, which include (i) no chemical reaction between the bitumen and the gas, (ii) isothermal conditions throughout the pressure-decay experiment, (iii) a constant value of diffusion coefficient, (iv) a constant gas compressibility factor, (v) the bitumen being nonvolatile, (vi) negligible swelling of the bitumen, (vii) and thermodynamic equilibrium at the gas/bitumen interface, as described by Henry's law. The errors associated with two main assumptions, namely, (iv) and (vi), are estimated later.

The two models developed in this study are the finite-acting model and the infinite-acting model. The diffusivity coefficient is obtained from the infinite-acting model. The finite-acting model is used to determine the time beyond which the use of the infinite-acting model would lead to large uncertainties in the estimated diffusion coefficient values.

The Infinite-Acting Model. As the gas diffuses into the bitumen, its penetration depth increases with time. The diffusion equations suggest that the penetration depth encompasses the total depth of the system at all times; however, at early times, there is little effect of diffusion beyond a particular depth, which is referred to as the penetration depth. Over the time interval before the penetration depth reaches the bottom of the pressure cell, the actual location of the bottom of the cell would be irrelevant, and it may be assumed to be infinity.

The aforementioned treatment is analogous to the infinite-acting behavior of pressure diffusion in petroleum reservoirs under single-phase flow conditions. There, the penetration depth is called the "radius of investigation".[17] The development in this section is for the early-time infinite-acting period, before the closed boundary at the cell bottom starts to influence the gas diffusion in bitumen.

With the assumptions stated previously, the diffusion of gas into the bitumen can be modeled by Fick's second law of diffusion:

$$D\frac{\partial^2 C}{\partial z^2} = \frac{\partial C}{\partial t} \tag{1}$$

For the gas-free bitumen samples used in pressure-decay experiments,[11,12] the initial condition is

$$C = 0 \qquad z \geq 0, t = 0 \tag{2}$$

The interface boundary condition is modeled based on two criteria. First, the interface between the gas and the bitumen is at equilibrium at $t > 0$. Second, the mass of the diffused gas is equal to the difference between the initial mass of the gas and the mass of the remaining gas in the pressure cell. In a mathematical form, this mass balance can be written as

$$m_d = \frac{VM}{RT}\left[\frac{P_i}{Z_i} - \frac{P}{Z}\right] \tag{3}$$

Assuming Z to be constant, eq 3 is differentiated to find the mass rate of gas diffused into the bitumen:

$$\frac{dm_d}{dt} = -\frac{VM}{ZRT}\frac{dP}{dt} \tag{4}$$

The mass rate of gas diffused can also be calculated from Fick's first law of diffusion:

$$\frac{dm_d}{dt} = -DA\frac{\partial C}{\partial z}\bigg|_{z=0} \tag{5}$$

Equating eqs 4 and 5 yields the interface boundary condition:

$$DA\frac{\partial C}{\partial z} = \frac{VM}{ZRT}\frac{dP}{dt} \qquad z = 0, t > 0 \tag{6}$$

The concentration of the gas in the bitumen at the interface, where the two phases are at equilibrium, can be expressed in term of pressure using Henry's law,[18] as follows:

$$P = K_h C \tag{7}$$

By combining eqs 6 and 7, the interface boundary condition takes the following form:

$$DA\frac{\partial C}{\partial z} = \frac{VMK_h}{ZRT}\frac{dC}{dt} \qquad z = 0, t > 0 \tag{8}$$

During early times, before the closed boundary at the cell bottom affects the rate of mass transfer between the gas and the bitumen, an infinite-acting boundary condition can be assumed:

$$C = 0 \qquad z \rightarrow \infty, t > 0 \tag{9}$$

The validity of the aforementioned boundary condition will be examined later. The mathematical formulation, given by eqs 1, 2, 8, and 9, was solved using the method of Laplace transform. The analytical solution obtained is[19]

$$C(z,t) = \frac{P_i}{K_h}\exp\left[\frac{z}{c_1 D}\right]\exp\left[\left(\frac{1}{c_1\sqrt{D}}\right)^2 t\right]\operatorname{erfc}\left(\frac{\sqrt{t}}{c_1\sqrt{D}} + \frac{z}{2\sqrt{Dt}}\right) \tag{10}$$

where $c_1 = (LMK_h)/(DZRT)$. Equation 10 gives the concentration of the diffusing gas in the bitumen as a function of depth and time. By evaluating eq 10 at the interface ($z = 0$), in conjunction with Henry's law, the expression for the gas phase (or cell) pressure is

$$P(t) = P_i \exp\left(\frac{\sqrt{D}ZRT\sqrt{t}}{LMK_h}\right)^2 \operatorname{erfc}\left(\frac{\sqrt{D}ZRT\sqrt{t}}{LMK_h}\right) \tag{11}$$

The aforementioned relationship is the forward solution

(17) Matthews, C. S.; Russell, D. G. *Pressure Buildup and Flow Tests in Wells*; Monograph Series VI; Society of Petroleum Engineers: Dallas, TX, 1967; pp 116−117.

(18) Felder, R. M.; Rousseau, R. W. *Elementary Principles of Chemical Processes*; Wiley: New York, 1986.

(19) Sheikha, H. Analytical Methods for Determination of the Gas Diffusivity Coefficient in Bitumen. Department of Chemical and Petroleum Engineering, University of Calgary, Calgary, Alberta, Canada, 2004.

for the gas-phase pressure as a function of time, which requires the values of all other variables, including the diffusivity coefficient. An inverse solution method for obtaining the diffusivity coefficient from eq 11 will be derived later.

Equation 11 suggests that pressure in the gas zone is a function of the square root of the diffusion coefficient divided by Henry's constant. Therefore, the analysis of the pressure-decay data will result in $\sqrt{D}/K_h$. This is an important observation and suggests that the early-time data do not contain enough information to allow independent estimation of both the Henry's constant and the diffusion coefficient. However, this is not a major drawback. An independent estimation of Henry's constant for gas−bitumen mixtures can be obtained from the gas-solubility data. As shown later, existing gas-solubility correlations for Athabasca bitumen were used for an independent estimation of Henry's constant. More discussion related to the consequences of this observation is given later. In the following, we will use eq 11 to develop an inverse method for the determination of $\sqrt{D}/K_h$.

The Finite-Acting Model. As mentioned previously, the finite-acting model was developed to determine the time beyond which the assumption of the infinite-acting boundary condition would not be valid. In the finite-acting model, the second boundary condition at the cell bottom is

$$\frac{\partial C}{\partial z} = 0 \qquad z = H,\ t > 0 \tag{12}$$

The analytical solution of the finite-acting model, consisting of eqs 1, 2, 8, and 12 in the Laplace domain is given by the following equation:[19]

$$P(s) = \frac{c_1 P_i \left[1 + \exp\left(-2H\sqrt{\frac{s}{D}}\right)\right]}{\left(c_1 s + \sqrt{\frac{s}{D}}\right) + \left[\left(c_1 s - \sqrt{\frac{s}{D}}\right)\exp\left(-2H\sqrt{\frac{s}{D}}\right)\right]} \tag{13}$$

where s denotes the Laplace transform variable. Numerical solutions for the finite-acting model (eq 13) were obtained using the Stehfest algorithm.[20]

The Inverse Problem

Schulze-Riegert et al.[21] defined the inverse problem as one in which the measured data can be reproduced on the basis of unknown model parameters. In other words, the solution of the inverse problem allows the unknown causes to be determined based on the observation of their effects. The inverse problem can be classified based on the type of information being sought in the solution procedure. When the initial condition needs to be determined, the inverse problem is called the backward problem. If a constant multiplier in the governing equation must be found, the inverse problem is called the coefficient inverse problem. The pressure-decay problem in the present study belongs to the latter class of inverse problems; i.e., it is the coefficient inverse problem.

Table 1. Summary of Gas−Bitumen Pressure-Decay Experiments[a]

pressure-decay experiment	gas	temp (°C)	P_i (MPa)	P_f (MPa)	duration (h)	H (m)
run 1	CH_4	75	4.02	3.69	53	0.0105
run 2	CH_4	90	4.05	3.76	22	0.0106
run 3	N_2	75	4.08	3.97	55	0.0113
run 4	N_2	90	4.05	3.93	39	0.0114
run 5	CO_2	75	4.00	3.24	42	0.0101
run 6	CO_2	90	3.96	3.42	20	0.0096

[a] Data taken from refs 11 and 12.

We seek the development of a technique for the determination of $\sqrt{D}/K_h$, hereafter called the combination factor, by analyzing the measured gas pressure values with time. Note that a similar situation is encountered in petroleum engineering that involves estimation of the reservoir permeability by measuring the pressure change in the well-bore. The governing equation involved in the propagation of pressure is the diffusivity equation of single-phase fluid flow in the radial direction. In well-testing, many of the available methods use an analytical forward solution to develop an inverse solution to determine the physical properties of interest. Techniques have been developed for identifying a portion of the data that follows the ideal forward solution. A class of successful techniques that were developed in the 1980s is based on graphical representation of a special derivative of the pressure data to allow a clear identification of the flow regimes.

In this study, a graphical approach is developed that is analogous to that used in well-testing for the determination of reservoir permeability.[22] In the graphical technique, the pressure, or its derivative, is plotted on certain coordinates and the permeability is found from the resulting plot. The advantage of the graphical derivative techniques is that they allow the identification of portions of the data that are affected by processes that are not included in the forward model. For the diffusion problem, if the data at early times were affected by pressure effects or if the later-time data were affected by the closed boundary, the graphical representation of the data would allow the identification of such data for their exclusion from calculations. Two such graphical techniques are presented in the following section.

The data from six pressure-decay tests[11,12] were subjected to the inverse solution methodology derived from eq 11. These tests, which are referred to as runs 1−6, involved methane, nitrogen, and carbon dioxide diffusing into bitumen at temperatures of 75 and 90 °C.[11,12] The experimental conditions of these six pressure-decay runs are summarized in Table 1. The diffusivity coefficients are obtained for these tests and compared with published values.

Graphical Method I. An explicit expression for the combination factor could not be derived, because of the nonlinearity of the functional relationship in eq 11. The

(20) Stehfest, H. Algorithm 368, Numerical Inversion of Laplace Transforms. *Commun. ACM* **1970**, *13*, 47.

(21) Schulze-Riegert, R. W.; Haase, O.; Nekrassov, A. Combined Global and Local Optimization Techniques Applied to History Matching. Presented at SPE Reservoir Simulation Symposium, Houston, TX, February 3−5, 2003, SPE Paper No. 79668.

(22) Mattar, L. Derivative Analysis Without Type Curves. *J. Can. Pet. Technol.* **1999**, *38* (13), Paper 97-51 (6 pp). (Special Edition CD-ROM.)

magnitudes of both the complementary error function term and the exponential term in eq 11 were compared, which showed that the exponential term remains close to unity. This observation allowed an approximate estimate of the combination factor. Thus, in developing Graphical Method I, we ignored the exponential term in eq 11 altogether. Equation 11 was rearranged and differentiated with respect to $\sqrt{t}$, which resulted in the following expression:

$$\frac{\mathrm{d}[\mathrm{erfc}^{-1}\{P(t)/P_\mathrm{i}\}]}{\mathrm{d}(\sqrt{t})} = \frac{\sqrt{D}ZRT}{K_\mathrm{h}LM} \tag{14}$$

We will refer to the left-hand side of eq 14 as the derivative function. Note that eq 14 represents a flat line on a graph of $\mathrm{d}[\mathrm{erfc}^{-1}\{P(t)/P_\mathrm{i}\}]/\mathrm{d}(\sqrt{t})$ versus t, from which the combination factor could be obtained from the intercept with the ordinate. The intercept, which is denoted as b, is equal to $\sqrt{D}\,ZRT/K_\mathrm{h}LM$. After the value of b has been determined graphically, the combination factor can be obtained from the following:

$$\frac{\sqrt{D}}{K_\mathrm{h}} = \left(\frac{LM}{ZRT}\right)b \tag{15}$$

The results with the estimated value of the combination factor indicated that the exponential term in eq 11 made a small contribution to the predicted pressure-decay profiles.[19]

Graphical Method II. In this method, the exponential term in eq 11 is not ignored. That is, Graphical Method II is developed by taking the derivative of the pressure equation (eq 11), with respect to time, i.e.,

$$\frac{\mathrm{d}P(t)}{\mathrm{d}t} = P_\mathrm{i}\left[\left(\frac{\sqrt{D}ZRT}{LMK_\mathrm{h}}\right)^2 \mathrm{erfc}\left(\frac{\sqrt{D}ZRT\sqrt{t}}{LMK_\mathrm{h}}\right) \exp\left(\frac{\sqrt{D}ZRT\sqrt{t}}{LMK_\mathrm{h}}\right)^2 - \frac{\sqrt{D}ZRT}{LMK_\mathrm{h}\sqrt{\pi t}}\right] \tag{16}$$

Combining eq 16 with eq 11 leads to the following relationship:

$$\frac{1}{P(t)}\frac{\mathrm{d}P(t)}{\mathrm{d}t} = \left(\frac{\sqrt{D}ZRT}{LMK_\mathrm{h}}\right)^2 - \left(\frac{\sqrt{D}ZRT}{LMK_\mathrm{h}\sqrt{\pi}}\right)\frac{P_\mathrm{i}}{P(t)\sqrt{t}} \tag{17}$$

Equation 17 suggests that, if the pressure-decay data are plotted as $(1/P(t))\mathrm{d}P(t)/\mathrm{d}t$ on the ordinate and $P_\mathrm{i}/[P(t)\sqrt{t}]$ on the abscissa, a straight line should be obtained over the infinite-acting period. The combination factor can be calculated from the slope of this straight line, m, as shown below:

$$\frac{\sqrt{D}}{K_\mathrm{h}} = -\left(\frac{LM\sqrt{\pi}}{ZRT}\right)m \tag{18}$$

Note that the combination factor could also be obtained from the square root of the intercept of the straight line corresponding to eq 17. However, it was determined that the resulting combination factor value was more sensitive to the intercept, because of the square function in eq 17.

Estimation of Henry's Constant. As mentioned previously, the use of pressure-decay data with both graphical methods based on eq 11 (namely, eqs 14 and 17) would result in the combination factor, which is a ratio of the square root of the diffusion coefficient and Henry's constant. Hence, an independent evaluation of the Henry's constant is necessary for determining the diffusion coefficient. In the present study, the Henry's constant value for each gas was calculated from a correlation for the volume-basis gas solubility, R_s (given in units of $\mathrm{m^3/m^3}$), in Athabasca bitumen.[23] The volume-basis gas solubility was converted to an average value of Henry's constant, using the following relationship:

$$K_\mathrm{h} = \frac{\bar{P}}{R_\mathrm{s}\rho_\mathrm{g}} \tag{19}$$

With the calculated value of Henry's constant, the diffusivity coefficient was determined from the combination factor determined previously.

Results and Discussion

Before describing the results from the two graphical methods for estimating the diffusivity coefficient of gases in bitumen, the magnitude of errors introduced by the three main assumptions is put under further investigation.

Evaluation of Assumptions. As mentioned previously, the mathematical formulation presented here ignored the effect of bitumen swelling, assumed a constant compressibility factor, and assumed that the closed boundary at the bottom of the vessel could be replaced by an infinite-acting boundary condition. These assumptions are examined in the following subsections.

Bitumen Swelling. The effect of neglecting the bitumen swelling is examined by calculating the swelling factor for all six runs. The swelling factor is defined as the ratio of the volume of bitumen at any time divided by the initial bitumen volume. The bitumen volume was found by calculating the mass fraction of gas dissolved in the bitumen, which was then used to estimate the bitumen density from the correlations reported by Svrcek and Mehrotra.[24]

The result showed that the variations in the calculated swelling factor for runs 1 and 2 with methane were 1.009 (after 50 h) and 1.007 (after 22 h), respectively. Knowing that the gas volume in the pressure cell was approximately twice that of the bitumen volume,[11,12] the aforementioned swelling factors were used to estimate the effect of swelling. The error in the estimated diffusion coefficient due to ignoring the effect of bitumen swelling was estimated to be 5.9% for run 1 and 5.5% for run 2. Table 2 lists the relative errors for all of the experiments at 30 h. The relative errors are the greatest for runs 5 and 6 with carbon dioxide.

The formulation of the problem incorporating the interface movement leads to a diffusion convection equation where the magnitude of the convective term is proportional to interface velocity. On the other hand,

(23) Mehrotra, A. K.; Svrcek, W. Y. Correlations for Properties of Bitumen Saturated with CO_2, CH_4 and N_2, and Experiments with Combustion Gas Mixtures. *J. Can. Pet. Technol.* **1982**, *21* (6), 95.

(24) Svrcek, W. Y.; Mehrotra, A. K. Gas Solubility, Viscosity and Density Measurements for Athabasca Bitumen. *J. Can. Pet. Technol.* **1982**, *21* (4), 31.

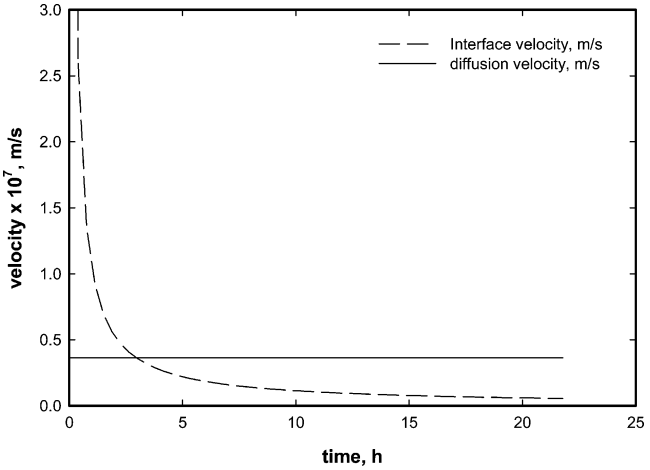

Figure 1. Comparison of the gas/bitumen interface velocity and diffusion velocity for run 1.

Table 2. Estimation of Relative Errors in Predicted Pressures due to Neglecting Bitumen Swelling and the Constant Gas Compressibility Factor

		relative error (%)		
gas	temp (°C)	due to neglecting bitumen swelling	due to constant gas compressibility factor	combined relative error
CH_4	75	5.9	1.3	7.2
CH_4	90	5.5	1.0	6.5
N_2	75	8.4	−0.1	8.3
N_2	90	8.0	−0.2	7.8
CO_2	75	9.3	4.8	14.1
CO_2	90	8.5	4.3	12.8

the magnitude of the diffusion term is proportional to *D*/*L*. The convective term may be ignored when the velocity of the interface is less than *D*/*L*. Figure 1 compares the velocity of the gas/bitumen interface with the diffusion velocity, indicating that the diffusion velocity is higher than the interface velocity. This confirms that the process is dominated by diffusion. The interface velocity is higher only at early times, and this portion of the data was not included in the calculation of the combination factor.

Constant Compressibility Factor. The gas compressibility factor for each gas was calculated from the Peng−Robinson[25] equation of state, to verify the validity of assuming this factor to be constant. For the experimental conditions of runs 1 and 2, the gas compressibility factor was determined to vary by <0.4%, as shown in Figure 2. The relative error in the calculated pressure values due to the constant gas compressibility factor assumption was estimated, and the results are summarized in Table 2. Again, the relative error is the greatest for runs 5 and 6 with carbon dioxide. The combined error for the calculated pressure for the CO_2−bitumen system, because of the assumptions related to bitumen swelling and the gas compressibility factor, was ∼13%−14%.

Infinite-Acting Assumption. The method of finding the combination factor relies on the solution to the infinite-acting problem, while the physical problem is finite. The infinite-acting time was determined from plotting both the finite-acting and infinite-acting results. Figure 3 shows the variation of pressure profile for runs 1 and 5 with both models. For the first 24 h, both models gave

(25) Peng, D.-Y.; Robinson, D. B. A New Two-Constant Equation of State. *Ind. Eng. Chem. Fundam.* **1976**, *15*, 59.

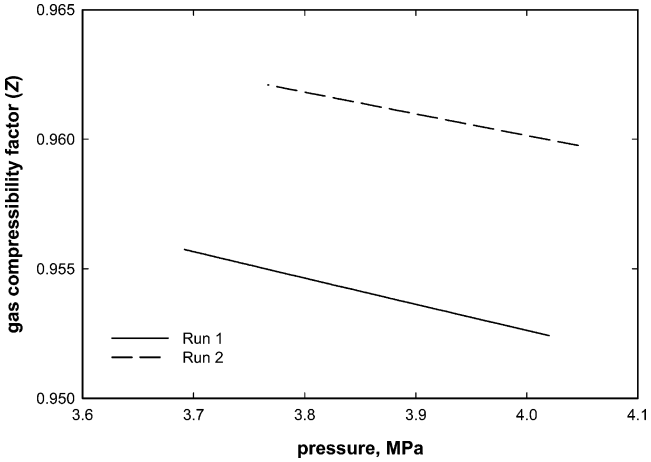

Figure 2. Variation in the gas compressibility factor for methane for runs 1 and 2.

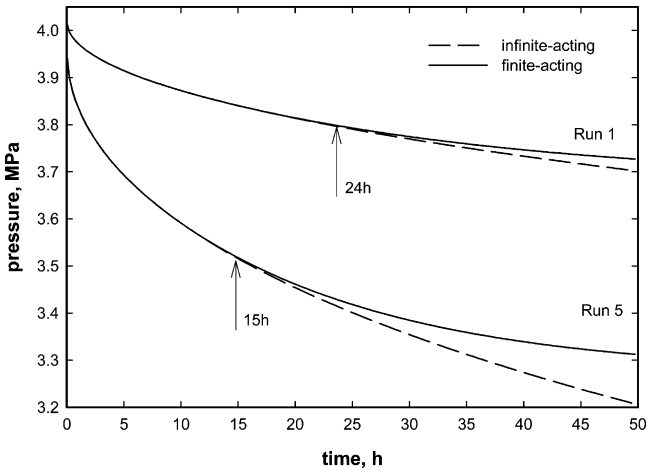

Figure 3. Predicted pressure-decay profiles from finite-acting and infinite-acting models for runs 1 and 5.

the same results for run 1. The diffusivity coefficient was estimated from the pressure-decay measurements during this period. For run 5, however, the infinite-acting model started to deviate from the finite-acting model after ∼15 h. Similar comparisons were made for all experiments to estimate the infinite-acting period.[19] Thus, these graphical methods can distinguish between the infinite- and finite-acting period, making it unnecessary to estimate the infinite-acting period in advance of the analysis.

Estimation of the Diffusion Coefficient. In this section, we apply Graphical Methods I and II to obtain the combination factor for the diffusion coefficient of methane, nitrogen, and carbon dioxide in Athabasca bitumen. The combination factor was obtained from the portion of the data that indicated infinite-acting behavior. For Graphical Method I, the combination factor was obtained by plotting the experimental data in accordance with eq 14.

It was noted that the derivative function magnified the noise in the experimental data. To avoid this, the derivative function values were smoothened. The results at 75 and 90 °C, for all three gases, are shown in Figures 4 and 5, respectively. In each case, the derivative value was obtained from the slope of a best-fit line through several data points in the vicinity of a particular point. Although this procedure led to smooth curves, it has the

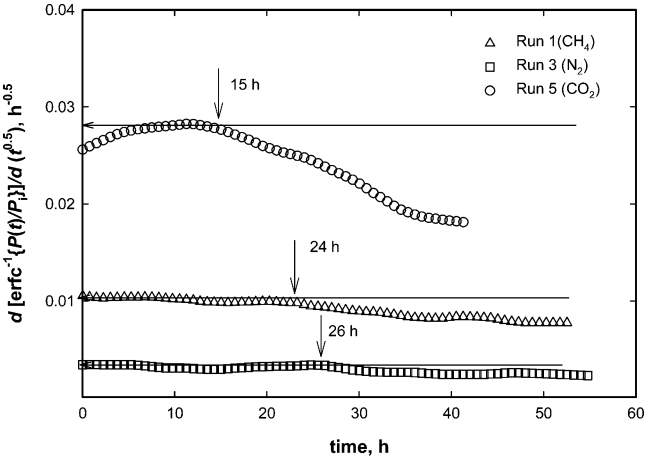

Figure 4. Estimation of the combination factor from early-time data using Graphical Method I for runs 1, 3, and 5 at 75 °C.

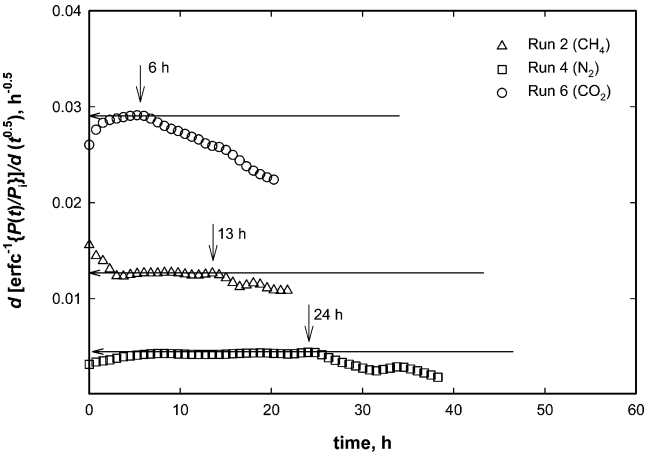

Figure 5. Estimation of the combination factor from early-time data using Graphical Method I for runs 2, 4, and 6 at 90 °C.

drawback that the data at one time affected the data at the next time. Note that a significant amount of early-time data in Figures 4 and 5 did not yield the expected "flat-line behavior". This was primarily because the early-time data, which are affected by fluctuations in experimental values, influenced the estimated value of the derivative function at subsequent times.

As seen in Figures 4 and 5, the end of the infinite-acting period can be determined from the derivative plot as the time that corresponds to a departure from the "flat-line behavior" in the derivative values. This departure suggested that the gas diffusing through the bitumen layer would have reached the bottom of the cell, such that it affected the cell pressure. Thus, the derivative value is seen to serve as a tool for identifying the end of the infinite-acting behavior, as well as for finding the combination factor from that portion of the data for which the infinite-acting assumption is valid. As mentioned previously, a similar methodology is adopted in petroleum reservoir well-testing, where the data affected by the outer-closed boundary is distinguished from the infinite-acting data. Figures 4 and 5 show how the derivative function at late times decreases because of the effect of the bottom of the cell. The times for the end of the infinite-acting behavior in Figures 4 and 5 correspond to those in Figure 3, as explained previously.

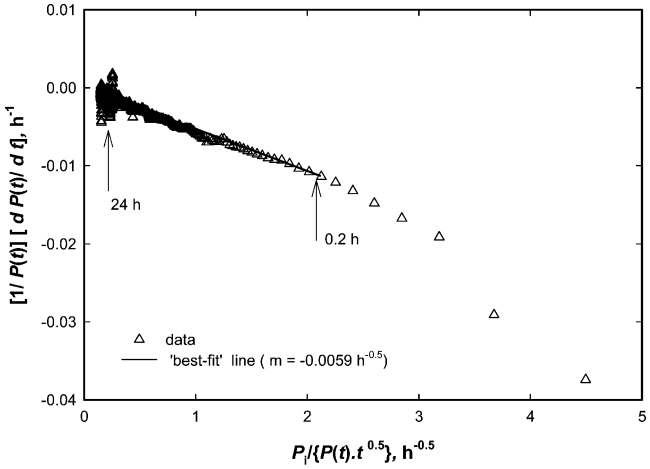

Figure 6. Estimation of the combination factor from late-time data using Graphical Method II for run 1 with CH_4.

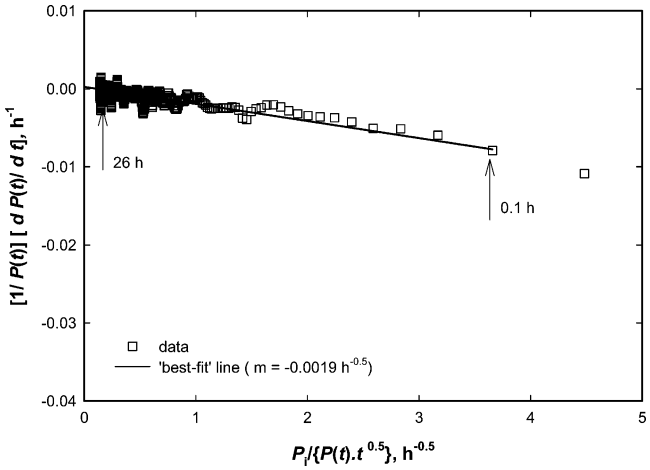

Figure 7. Estimation of the combination factor from late-time data using Graphical Method II for run 3 with N_2.

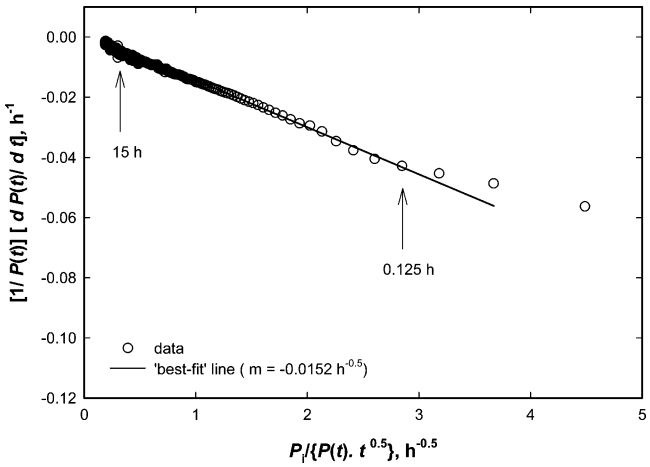

Figure 8. Estimation of the combination factor from late-time data using Graphical Method II for run 5 with CO_2.

The intercept of the straight line with the ordinate was obtained from Figures 4 and 5. Equation 15 was then used to calculate the combination factor.

For Graphical Method II, the experimental data of runs 1, 3, and 5 were plotted using eq 17. The results are shown in Figures 6–8. Similar to Graphical Method I, an important characteristic of this method involves identifying the portion of the data that does not follow the predictions from the mathematical model. For

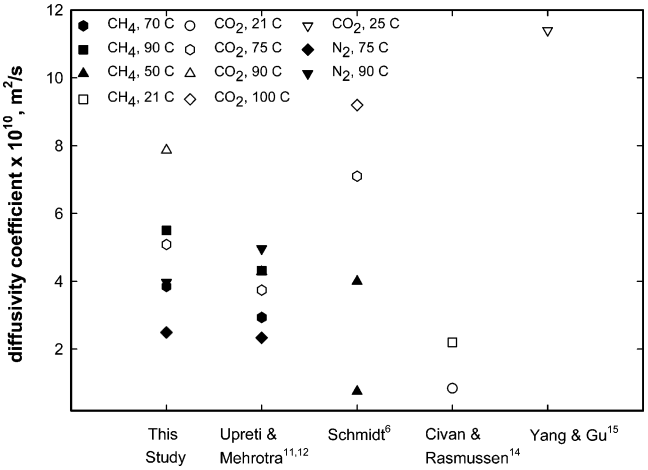

Figure 9. Comparison of diffusivity coefficients predicted from Graphical Methods I and II with literature data.

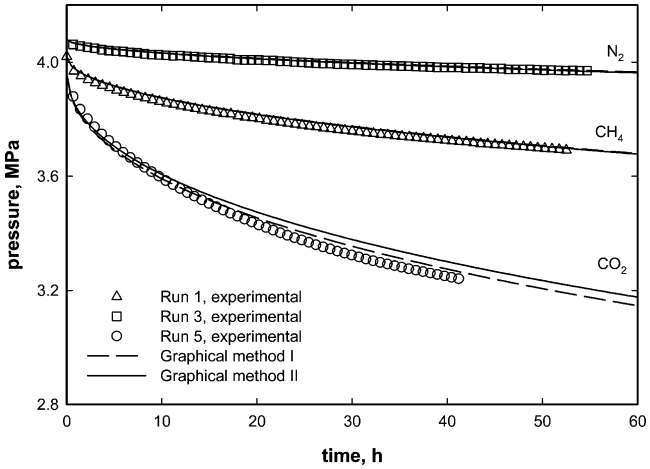

Figure 10. Reproduced and experimental pressure-decay curves for runs 1, 3, and 5 at 75 °C using predicted combination factors obtained from Graphical Methods I and II.

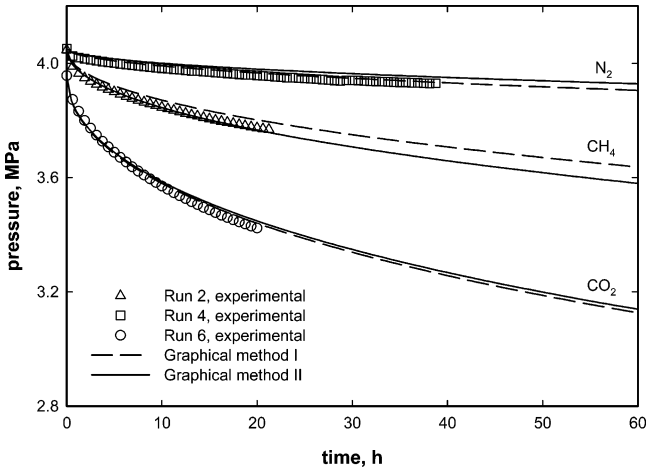

Figure 11. Reproduced and experimental pressure-decay curves for runs 2, 4, and 6 at 90 °C using predicted combination factors obtained from Graphical Methods I and II.

example, if the experimental data are affected by experimental fluctuations or are due to the closed boundary at the bottom of the cell, the data did not fall on the straight line and were not incorporated into the analysis. That is, only that part of data that followed the infinite-acting behavior and fell on a straight line was used for further analysis. After the slope (m) was determined, eq 18 was used to obtain the combination factor. As mentioned previously, Henry's constant was estimated from the calculated gas solubility, using eq 19. The calculated Henry's constant was then used, along with the estimated value of the combination factor to determine the diffusivity coefficient.

The diffusivity coefficient values obtained for the three gases are given in Table 3. In Figure 9, the diffusivity coefficient values from the two graphical methods are compared with those reported by other investigators.[6,11,12,14,15] The diffusivity coefficients from the two graphical methods are in agreement with the results by Schmidt et al.[6] and Upreti and Mehrotra.[11,12]

To further validate the results of this study, the pressure-decay profiles were generated by substituting all parameters in the forward solution (eq 11), including the predicted values of the combination factor. These reproduced pressure-decay profiles are plotted for all gases at 75 °C and 90 °C in Figures 10 and 11, respectively. The experimental pressure-decay data of Upreti and Mehrotra[11,12] are also plotted for comparison. Figures 10 and 11 show that the combination factors obtained from the two graphical methods gave a reasonable match of the experimental pressure-decay data.

Comparison of Graphical Methods I and II. As observed in Figures 10 and 11, the predicted pressure-decay profiles with the diffusion coefficients estimated from the two graphical methods are very similar, to the extent that one method cannot be concluded to be superior to the other. In Table 3, the predicted diffusion coefficients from the two graphical methods compare well for all gas−bitumen systems, and their values increase with temperature.

For a constant bitumen-layer thickness, the infinite-acting time period is inversely related to the magnitude of the diffusivity coefficient. The higher the diffusivity coefficient, the shorter the infinite-acting time period. For Graphical Method I, it is clear from Figures 4 and 5 that carbon dioxide has a shorter infinite-acting period, in comparison to that for nitrogen and methane. However, the results in Figures 6−8 for Graphical Method II do not show the end of the infinite-acting period. This is attributed to the $1/\sqrt{t}$ term in the

Table 3. Predicted Values of the Combination Factor and Diffusivity Coefficient for CH_4−Bitumen, N_2−Bitumen, and CO_2−Bitumen Systems at 4 MPa

experimental gas−bitumen system		Graphical Method I		Graphical Method II	
		$\sqrt{D}/K_h$ (kg Pa^{-1} m^{-2} s$^{-0.5}$)	D (m^2/s)	$\sqrt{D}/K_h$ (kg Pa^{-1} m^{-2} s$^{-0.5}$)	D (m^2/s)
run 1	CH_4 at 75 °C	1.17×10^{-6}	3.85×10^{-10}	1.18×10^{-6}	3.89×10^{-10}
run 2	CH_4 at 90 °C	1.35×10^{-6}	5.50×10^{-10}	1.56×10^{-6}	7.32×10^{-10}
run 3	N_2 at 75 °C	0.60×10^{-6}	2.49×10^{-10}	0.61×10^{-6}	2.60×10^{-10}
run 4	N_2 at 90 °C	0.73×10^{-6}	3.97×10^{-10}	0.61×10^{-6}	2.78×10^{-10}
run 5	CO_2 at 75 °C	9.72×10^{-6}	5.08×10^{-10}	9.29×10^{-6}	4.64×10^{-10}
run 6	CO_2 at 90 °C	9.64×10^{-6}	7.87×10^{-10}	9.47×10^{-6}	7.58×10^{-10}

independent variable for the plots, which has a tendency to stretch the early-time pressure-decay data and squeeze the late-time data.

Finally, the results presented in this paper suggest that the pressure-decay data collected during the early time do not have sufficient information to obtain both the diffusivity coefficient and Henry's constant. To estimate both of these independently from the same experiment, the pressure-decay runs could be conducted over longer time periods, such that the effect of the closed boundary is manifested significantly in the analytical solution. In this case, Henry's constant could be obtained from the late-time period, when the effect of mass diffusion decreases as the gas concentration in the entire bitumen sample approaches the solubility limit.

Conclusions

The analytical solution for the diffusion equation was obtained, leading to an inverse solution technique for developing a graphical approach for the estimation of diffusivity coefficient. The developed technique was used to estimate the diffusion coefficient of light gases (methane, nitrogen, and carbon dioxide) in Athabasca bitumen, using the pressure-decay data reported by Upreti and Mehrotra.[11,12] Two graphical methods were developed, based on the infinite-acting and finite-acting boundary conditions. The analytical solution of the forward problem, as presented in this study, suggested that the infinite-acting pressure-decay data do not include sufficient information to allow simultaneous estimation of the diffusion coefficient and Henry's constant for the bitumen gas-solubility at equilibrium. Because of the coupling of the diffusion coefficient and Henry's constant in the combination factor, independent measurements of the gas solubility of the bitumen were used to estimate the diffusion coefficient.

The graphical methods are simple to use. The estimated diffusivity coefficients for gas−bitumen pairs varied over a range of 2.5×10^{-10}−7.8×10^{-10} m^2/s. These results for the diffusion coefficient were shown to be in agreement with the range of values reported previously. Furthermore, the graphical methods allowed the identification of portions of the data that were affected by experimental fluctuations. Based on this information, the diffusion coefficient values were obtained by considering only that portion of the data that was consistent with the analytical solution.

Acknowledgment. Financial support from the Natural Sciences and Engineering Research Council of Canada (NSERC) and the Department of Chemical and Petroleum Engineering at the University of Calgary is gratefully acknowledged. We thank Simant R. Upreti (presently at Ryerson University, Toronto, Canada) for providing the pressure-decay data used in this study.

Nomenclature

A = cross-sectional area of the pressure cell (m^2)
b = intercept of the straight line in Graphical Method I
C = concentration of gas in bitumen (kg/m^3)
D = diffusivity coefficient (m^2/s)
K_h = Henry's constant (Pa m^3/kg)
H = thickness of bitumen layer in the pressure cell (m)
L = height of gas zone in the pressure cell; $L = 0.03 - H$ (m)
M = molar mass of gas (kg/kmol)
m = slope of the straight line in Graphical Method II
m_d = mass of gas diffused in bitumen (kg)
P = pressure (Pa)
$\bar{P}$ (s) = pressure term in the Laplace domain
$\bar{P}$ = average pressure (Pa)
R = universal gas constant; $R = 8314$ J kmol^{-1} K^{-1}
R_s = volume-basis solubility of gas in bitumen (m^3(at 0 °C and 101.3 kPa)/m^3)
s = Laplace transform variable
t = time (s)
T = temperature (°C or K)
V = volume of gas (m^3)
z = depth (m)
Z = gas compressibility factor

Subscripts

f = final value
i = initial value

Greek Symbols

ρ_g = gas density (kg/m^3)

Acronyms

SCF = Suncor's Coker Feed bitumen sample
SYN = Syncrude bitumen sample

EF050057C